Published in final edited form as:
Hear Res. 2008 December ; 246(1-2): 1–8. doi:10.1016/j.heares.2008.09.004.

Distribution of two-pore-domain potassium channels in the adult rat vestibular periphery

Paul Popper[†,‡,¥], **John Winkler**[†,¥], **Christy B. Erbe**[†], **Alexandara Lerch-Gaggl**[‡], **Wolfgang Siebeneich**[†], and **P. Ashley Wackym**[*,†,§]

†*Department of Otolaryngology and Communication Sciences, Medical College of Wisconsin, 9200 West Wisconsin Avenue, Milwaukee, WI 53226, USA*

§*Department of Physiology, Medical College of Wisconsin, 9200 West Wisconsin Avenue, Milwaukee, WI 53226, USA*

‡*Department of Cell Biology, Anatomy and Neurobiology, Medical College of Wisconsin, 9200 West Wisconsin Avenue, Milwaukee, WI 53226, USA*

Abstract

Constitutively active background or “leak” two-pore-domain potassium (K^+) channels (Kcnk family), as defined by lack of voltage and time dependency are central to electrical excitability of cells by controlling resting membrane potential and membrane resistance. Inhibition of these channels by several neurotransmitters, e.g. glutamate, or acetylcholine, induces membrane depolarization and subsequent action potential firing as well as increases membrane resistance amplifying responses to synaptic inputs. In contrast, their opening contributes to hyperpolarization. Because of their central role in determining cellular excitability and response to synaptic stimulation, these channels likely play a role in the differential effects of vestibular efferent neurons on afferent discharge. Microarray data from previous experiments showed Kcnk 1,2,3,6,12 and 15 mRNA in Scarpa’s ganglia. Real-time RT-PCR showed Kcnk 1,2,3,6,12 and 15 mRNA expression in Scarpa’s ganglia and Kcnk 1,2,3,6,12 but not 15 mRNA expression in the crista ampullaris. We studied the distribution of two-pore-domain potassium channels K_{2P}1.1, 2.1, 3.1 and 6.1 like immunoreactivity (corresponding to Kcnk genes 1, 2, 3 and 6) in the vestibular periphery. K_{2P}1.1 (TWIK 1) immunoreactivity was detected along nerve terminals, supporting cells and blood vessels of the crista ampullaris and in the cytoplasm of neurons of the Scarpa’s ganglia. K_{2P}2.1 (TREK 1) immunoreactivity was detected in nerve terminals and transitional cells of the crista ampullaris, in the vestibular dark cells and in neuronal fibers and somata of neurons of Scarpa’s ganglia. K_{2P}3.1 (TASK 1) immunoreactivity was detected in supporting cells and transitional cells of the crista ampullaris, in vestibular dark cells and in neuron cytoplasm within Scarpa’s ganglia. K_{2P}6.1 (TWIK 2) immunoreactivity was detected in nerve terminals, blood vessels hair cells and transitional cells of the crista ampullaris and in the somata and neuron fibers of Scarpa’s ganglia.

*Corresponding author. Department of Otolaryngology and Communication Sciences, Medical College of Wisconsin, 9200 W Wisconsin Avenue, Milwaukee, WI 53226-3596, USA. Tel.: +1.414.805.5582; fax: +1.414.805.8324. *E-mail address:* wackym@alumni.vanderbilt.edu (P. A. Wackym).
¥Joint first author.

Keywords

Inner ear; Kcnk; 2P-domain K^+ channel; Real Time RT-PCR, Immunohistochemistry; Confocal microscopy; Vestibular

1. Introduction

Leak or background potassium (K^+) channels are potassium selective channels that are relatively voltage independent and non-inactivating (see Honore, 2007; Krapivinsky et al., 1995; Lesage et al., 2000 for review). Since they can be opened independent of the membrane potential, these channels are central in setting the resting membrane potential and membrane conductance of cells and therefore, in excitable cells such as neurons, the response to synaptic input. Inhibition of these channels causes membrane depolarization and subsequent action potential firing as well as increases membrane resistance amplifying responses to synaptic input (Charpak et al., 1990; Nicoll et al., 1990). In contrast, their activation contributes to hyperpolarization.

Leak K^+ channels are inhibited by neurotransmitters active in the vestibular periphery such as glutamate through class 1 metabotropic glutamate receptors (Chemin et al., 2003; Talley et al., 2000) or acetylcholine through M3 muscarinic receptors (Millar et al., 2000). In addition, these K^+ channels are activated or inhibited by a wide variety of mechanisms (Lesage et al., 2000; Patel and Honore, 2001) such as physiological increase or decrease of intra- or extra-cellular pH (Duprat et al., 1997; Honore, 2007; Lesage et al., 1996; Maingret et al., 1999; Reyes et al., 1998), unsaturated fatty acids (Honore, 2007; Lauritzen et al., 2000), membrane stretch (Maingret et al., 1999), volatile anesthetics (Heurteaux et al., 2004; Patel et al., 1999; Rajan et al., 2001; Terrenoire et al., 2001), variations in temperature (Kang et al., 2005; Maingret et al., 2000) or oxygen tension (Miller et al., 2005; Rajan et al., 2001). Thus, these channels are important loci of modulation of the output of the inner ear by a variety of endogenous and exogenous agents and may be the molecular substrate of direct effect of temperature (von Baumgarten et al., 1984), pH (Vega et al., 2003) or increased endolymphatic pressure on the vestibular afferent discharge.

In addition to their potential role in shaping the vestibular afferent discharge, leak K^+ channels may play a role in endolymph homeostasis. Two leak channels, $K_{2P}1.1$ (Nicolas et al., 2003) and $K_{2P}2.1$ (Nicolas et al., 2004) have been described in the vestibular periphery and localized to the vestibular dark cells, suggesting they may play a role in potassium recycling.

Leak K^+ channels are dimers of two-pore-domain K^+ channels subunits. To date, 14 two-pore K^+ channel subunit genes have been found in mammals that form a family of K^+ channels designated by the Human Genome Project as KCNK genes. These channels have had different nomenclatures including $K_{2P}1.1$ to $K_{2P}17.1$, designated by the International Union of Pharmacology, corresponding to genes KCNK 1 to 17, excluding number 8, 11 and 14 in the order they were discovered. Other nomenclatures grouped the channels by sequence homology and sensitivities to physical characteristics such as pH, temperature, lipids, volatile anesthetics, membrane stretch, etc (Goldstein et al., 2005; Lesage et al., 2000; Patel and Ladzunski, 2004; Talley et al., 2003). We will refer to the K_{2P} nomenclature for the two-pore-domain K^+ channels and Kcnk for the two-pore-domain K^+ channel genes.

Previous microarray studies, of neurons in Scarpa's ganglion using laser capture microdissection and a chip that contained Kcnk1, 2, 3, 6, 9, 10, 12, 13 and 15 (Genus BioSystems, Inc., Northbrook, IL), indicated that the two-pore-domain K^+ channels expressed in Scarpa's ganglia are Kcnk1, 2, 3, 6, 12 and 15 (GEO accession GSE4458 and GSE9684;

[Wackym, 2008]). In this study, we determined the expression of these two-pore-domain K^+ channel genes, through real time PCR and the distribution of four of their proteins (K_{2P}1.1, 2.1, 3.1, 6.1) immunoreactivities in the vestibular periphery. We used anti myosin VIIA, tubulin β III and calretinin antibodies to identify hair cells and nerve terminals, respectively, in the cristae ampullares. Myosin VIIA is a non-muscle isoform of myosin expressed only in hair cells in the vestibular periphery (Hasson et al., 1997). Tubulin β III is expressed specifically in neurons (Jiang and Oblinger, 1992) and calretinin is a calcium binding protein that is only in calyx afferents (and in rats and mice in a few type II hair cells) (Dechesne et al., 1991; Desai et al., 2005; Leonard and Kevetter, 2002). The genes and channel subunits studied are shown in Table 1, including contemporary and past nomenclatures.

2. Materials and Methods

2.1 Animals

This study was performed in accordance with the United States Public Health Service Policy on Humane Care and Use of Laboratory Animals, the *NIH Guide for the Care and Use of Laboratory Animals*, and the Animal Welfare Act (7 U.S.C. §§2131 et seq.); the animal use protocol was approved by the Institutional Animal Care and Use Committee of the Medical College of Wisconsin.

2.2 RNA extraction and real-time reverse transcription-PCR

Twenty adult female Brown Norway rats were anesthetized with Nembutal sodium solution 55 mg/kg given by intraperitoneal injection. The rats were then decapitated. Scarpa's ganglia and crista ampullares were dissected out with an operating microscope and frozen at −80 °C. Total RNA was extracted from Scarpa's ganglia and cristae ampullares of 40 temporal bones using the TRIZOL® reagent (Invitrogen, Carlsbad, CA) according to their protocol, treated with RNase free DNase (RQ1, 1μl/20μl reaction, Promega) and then reverse transcribed (RT) using random hexamers (Omniscript, Qiagen, Hombrechtikon, Switzerland) with (RT positive) or without (RT negative) the addition of the reverse transcriptase.

Real-time RT-PCR was performed to show relative expression levels of the six K_{2P} channels expressed in the microarray in cristae and ganglia. Hypoxanthine guanine phosphoribosyl transferase (HPRT) was used as a reference gene as it has constant expression levels in the two tissues. RNA extracts from Scarpa's ganglia and cristae ampullares were treated with DNase I, Amp Grade (Invitrogen) then RT with random primers (Invitrogen) and Omniscript Reverse Transcription kit (Qiagen, Valencia, CA). Real-time RT-PCR was done with TaqMan® Gene Expression Assays (Applied Biosystems, Foster City, CA) for Kcnk1 (ABI: Rn00572452_m1), Kcnk2 (ABI: Rn01643939_m1), Kcnk3 (ABI: Rn00583727_m1), Kcnk6 (ABI: Rn00821542_g1), Kcnk12 (ABI: Rn02132664_s1), Kcnk15(ABI: Rn02349659_m1), and HPRT (ABI: Rn01527840_m1). Real-time PCR was performed on a iCyler iQ Multicolor Real-Time Detection System (Bio Rad Laboratories, Hercules, CA). Real-time reactions contained 10 μl 2x TaqMan® Universal PCR Master Mix (ABI, Foster City, CA), 1 μl of 20x TaqMan® Gene Expression Assay (ABI, Foster City, CA), and 9 μl cDNA in RNase-free water. The thermal cycling conditions were as follows: 50 °C hold for 2 min, 95 °C hold for 10 min, followed by two-step PCR for 45 cycles of 95 °C for 15 s and 60 °C for 1 min. An RT negative control was run for each channel and samples for Scarpa's ganglia and cristae ampullares were run in triplicate.

Within each experiment, the cycle threshold (C_T) for each of the triplicates for the potassium gene of interest and for the HPRT reference gene, in each tissue, was calculated and averaged. If the standard deviation of cycle threshold was greater than one cycle, that experiment was discarded. The C_T of HPRT was subtracted from the C_T of the potassium channels to generate

ΔC_T. Each experiment was run a total of three times and ΔC_T determined for each of the three runs. The ΔC_T from each of the three runs was averaged and the standard deviation calculated and reported in Table 2. The fluorescent tag that was used was FAM-490 (Biosearch Technologies, Novato CA).

2.3 Immunohistochemistry

Twenty male and female rats (young adult Brown Norway) were overdosed with sodium pentobarbital and perfused with 4% paraformaldehyde. The brains and temporal bones were removed. The crista ampullares and the Scarpa's ganglia were dissected out using an operating microscope and all harvested tissues were post-fixed for 1 hour in the same fixative. The crista ampullares and ganglia were embedded in 5% agarose in PBS. The agarose blocks were shaped into rectangles and placed in PBS until processing. Agarose blocks containing Scarpa's ganglion or vestibular crista ampullaris were cut in 40 μm sections on a vibratome and collected in 1X PBS. Primary antibodies were purchased from Chemicon (Temecula, CA; anti-$K_{2P}3$, anti-$K_{2P}6.1$ and anti-tubulin β III), Alomone Labs (Jerusalem, Israel; anti-$K_{2P}1.1$) and Santa Cruz Biotechnology (Santa Cruz, CA; Anti-$K_{2P}2.1$, anti calretinin and anti myosin VIIA). Blocking peptides came with all antibodies. Alexa-488 and Alexa-568 labeled secondary antibodies were purchased from Molecular Probes (Invitrogen Corporation, Carlsbad, CA). Horseradish peroxidase (HRP) labeled secondary antibodies were purchased from Jackson Laboratories (West Grove, PA).

Floating sections were washed 3 × 30 min in PBS and incubated in for 60 min in PBS containing 5% normal serum and 0.3% Triton X-100. Subsequently, sections were incubated for 48 hr at 4°C with primary antibody diluted in PBS (with 0.3% Triton X-100) containing 5% of the appropriate normal serum. The antibody-antigen complexes were visualized either using Alexa labeled secondary antibodies diluted 1:1000 in 0.1 M Tris (pH 8.0) and 0.3% Triton X-100 or with HRP labeled secondary antibodies diluted 1:200 in PBS and 0.3% Triton X-100 using 3,3'-diaminobenzidine tetrahydrochloride (DAB) as the chromogen. Finally, sections were washed 3×10 min in 0.1M TRIS pH 8.0, mounted on slides, dried at 37° C in a slide warmer and were cover slipped with gelmount (Biomeda, Oakland Ca) or dehydrated and cover slipped with Permount. This process was used in the control experiments using antibodies for pre-absorbed overnight at 4° C with their respective blocking peptides in a ratio of 10:1 control peptide:antibody.

Sections were analyzed with a Zeiss Axioskop 2 microscope (Jena, Germany) using epifluorescence illumination. For co-localization of antigens, double-stained sections were imaged with a TCS SP2 laser scanning confocal microscope (Leica Microsystems, Heidelberg, Germany).

3. Results

3.1. Real-time RT-PCR

Real-time PCR revealed that Kcnk1, 2, 3, 6, 12 and 15 were expressed in the Scarpa's ganglion, and Kcnk1, 2, 3, 6 and 12 were expressed in the crista ampullaris. The expression levels of these genes, relative to the expression of HPRT in the Scarpa's ganglion and in the crista ampullaris, was calculated as the average number of cycles needed to reach threshold compared to HPRT (mean ΔC_T) and are shown in Table 2.

3.2. Immunohistochemistry

We studied the $K_{2P}1.1$, $K_{2P}2.1$, $K_{2P}3.1$ and $K_{2P}6.1$ immunoreactivity ($K_{2P}1.1i$, $K_{2P}2.1i$, $K_{2P}3.1i$ and $K_{2P}6.1i$, respectively) in the Scarpa's ganglion and crista ampullaris. Figure 1 shows that $K_{2P}1.1i$, $K_{2P}2.1i$, $K_{2P}3.1i$ and $K_{2P}6.1i$ were present in Scarpa's ganglia and cristae

ampullares. The details of the distribution of each channel-immunoreactivity in the ganglia and cristae ampullares are presented below and are summarized in Table 2. At the time of these experiments, no commercial antibodies were available for $K_{2P}12.1$ or $K_{2P}15.1$ the expression products of Kcnk12 and Kcnk15, respectively.

$K_{2P}1.1$ immunoreactivity in the ganglion cells was present in the somata of all neurons with more intense immunoreactivity in the larger neurons. In the crista, we observed $K_{2P}1.1i$ in nerve terminals, visualized with an antibody against the neuronal marker tubulin β III, suggesting that $K_{2P}1.1i$ is in nerve terminals (Fig. 2). We did not observe $K_{2P}1.1i$ in hair cells, labeled with the specific marker myosin VIIA immunoreactivity, or in transitional cells. $K_{2P}1.1i$ was observed in supporting cells, identified by their shape and by elimination (not co-localized with myosin VIIA immunoreactivity) and dark cells.

$K_{2P}2.1$ immunoreactivity in the Scarpa's ganglion was observed in neuronal somata both large and small (Fig. 1). In the crista ampullaris, $K_{2P}2.1i$ was observed in nerve terminals, visualized with tubulin β III staining, transitional cells and dark cells (Fig. 3). Figure 3 shows $K_{2P}2.1i$ and Tubulin β III immunoreactivity co-localized in a section of a crista ampullaris.

$K_{2P}3.1$ immunoreactivity was detected in neuronal somata in Scarpa's ganglia, both large and small (Fig. 1). $K_{2P}3.1i$ was more intense in the large neurons that were also calretinin positive (Fig. 4), but $K_{2P}3.1i$ was not co-localized with calretinin immunoreactivity in the crista ampullaris (Fig. 4). In the crista ampullaris, $K_{2P}3.1i$ was present in supporting cells, particularly in their apical portion (Fig. 5). Figure 5 also shows $K_{2P}3.1i$ was not co-localized with tubulin β III immunoreactivity indicating that $K_{2P}3.1$ is not in nerve terminals in the sensory epithelia of the crista ampullaris. $K_{2P}3.1i$ was also observed in transitional cells and dark cells (Fig. 1).

$K_{2P}6.1$ immunoreactivity in Scarpa's ganglion was observed in all neuronal somata at very low levels. Figure 6 shows K_{2P} 6.1i co-localized with β III immunoreactivity, indicating that K_{2P} 6.1i is in nerve terminals, and with myosin VIIA, indicating $K_{2P}6.1i$ is in hair cells, in the crista ampullaris. In addition, $K_{2P}6.1i$ was observed in transitional cells (Fig. 1).

4. Discussion

In this study we showed, using real-time RT-PCR that Kcnk1, 2, 3, 6, 12 and 15 are expressed in the rat Scarpa's ganglia and that Kcnk1, 2, 3, 6 and 12 are expressed in the cristae ampullares. In addition, we used immunohistochemistry to study the distribution of Kcnk1, 2, 3 and 6 immunoreactivities in the vestibular periphery.

Real-time PCR data was quantified in terms of the difference of number of cycles to reach threshold (ΔC_T) for the gene of interest and a housekeeping gene (HPRT). We chose HPRT because its threshold cycle (C_T) was closest to the threshold cycle of the Kcnk genes in these tissues. ΔC_T is related monotonously to fold difference level of expression compared to the level of expression of HPRT ($2*\exp(-{-}\Delta C_T)$). Assuming that the amplification efficiency is the same for all genes that were investigated (indeed, the reported efficiency of all TaqMan® primer sets is 1), Table 2 shows the relative expression levels of these genes in the Scarpa's ganglion and in the cristae ampullares.

4.1 Comparison with other work

Kcnk1 expression in the rat vestibular periphery has been demonstrated previously (Nicolas et al., 2003) by reverse-transcriptase PCR (RT-PCR). In that study, $K_{2P}1.1i$ has been found in large neuronal somata in the ganglion and vestibular dark cells in the end organs. Our results, while confirming these results in the ganglia, are somehow different in the cristae ampullares, where we observed $K_{2P}1.1i$ in supporting cells and dark cells. The reason for this discrepancy

is not clear. These differences may be due to differences in the antibodies used in these studies or the age differences in the animals. Nicolas et al. used neonates and pups (oldest were 24 days old) while we used young adults (45 to 60 days old).

The current study confirmed the results of previous studies showing K_{2P}2.1i in neuron terminals, transitional epithelium and vestibular dark cells of the crista ampullaris, and in neuronal fibers and somata of neurons of Scarpa's ganglia (Nicolas et al., 2004).

Kcnk3 mRNA has been detected by RT-PCR in the cochlea in rats (Kanjhan et al., 2004). These authors observed K_{2P}3.1i in supporting cells, fibrocytes and glial cells in the cochlear nerve. Our results are somehow in agreement, as we observed K_{2P}3.1i in vestibular supporting cells. In addition, we also observed K_{2P}3.1i in Scarpa's ganglion neurons.

In contrast to the present results, Nicolas et al., 2003 failed to detect the expression of Kcnk6 mRNA in the ganglion or in end organs of neonate and young rats by RT-PCR. This could be due to age difference of the animals or differences in PCR primers. Consequently, they did not investigate K_{2P}6.1i in the vestibular periphery. Mhatre et al., 2004 showed that Kcnk6 mRNA is expressed in the mouse cochlea and that K_{2P}6.1i is predominantly in the stria vascularis. We detected K_{2P}6.1i in the vestibular transitional cells and in nerve terminals in the vestibular epithelia.

4.2 Functional correlates

Two-pore-domain channels have complex regulatory properties. K_{2P}1.1 is activated by activators of protein kinase C (PKC) and is inhibited by intracellular acidosis (Lesage et al., 1996). K_{2P}2.1 (see Honore, 2007; Lesage, 2003 for reviews) is activated by elevated temperature (Maingret et al., 2000), mechanical pressure applied to the cell membrane (Maingret et al., 1999), arachidonic acid and other polyunsaturated fatty acids (Lauritzen et al., 2000), volatile general anesthetics (Patel et al., 1999; Terrenoire et al., 2001) and by low intracellular pH (Maingret et al., 1999). K_{2P}2.1 is inhibited by G_q-coupled receptors such as group I metabotropic glutamate receptor or muscarinic acetylcholine receptor 3 (Chemin et al., 2003; Lesage, 2003), by G_s-coupled receptors (Fink et al., 1996; Patel et al., 1998) and by activators of PKC and protein kinase A (PKA). K_{2P}3.1 is very sensitive to external pH in a very narrow physiological range. It is inhibited by a slight acidosis and is activated by slightly elevated pH (Buckler et al., 2000; Duprat et al., 1997; Lesage et al., 2000). It is activated by volatile general anesthetics (Buckler et al., 2000; Patel et al., 1999) and activators of PKA. K_{2P}3.1 is inhibited by local anesthetics and by G_q-coupled receptors (Chemin et al., 2003; Lesage, 2003) and by the endocanaboid anadamide (Maingret et al., 2001). It is not affected by PKC. Finally, K_{2P}6.1 is inhibited by heat (Patel et al., 2000) and intracellular acidification (Chavez et al., 1999; Patel et al., 2000) and is activated by PKC activators (Chavez et al., 1999).

K_{2P}12.1 is silent when expressed in Xenopus oocytes. However, it is probably a functionally important K^+ channel since its gene, Kcnk12, is expressed highly in the brain, lung, kidney and stomach. It is 61.8% identical to K_{2P}13.1 and only 25–35% identical with other two-pore channels (Rajan et al., 2001). K_{2P}13.1 is activated by arachidonic acid and is inhibited by volatile anesthetics. K_{2P}15.1 is also silent when expressed in Xenopus oocytes, though a chimeric K_{2P}15.1/K_{2P}9.1 produces potassium currents (Goldstein et al., 2005; Kim and Gnatenco, 2001; Patel and Ladzunski, 2004). It is from the same family of two-pore channels as K_{2P}3.1 (Duprat et al., 2007; Kim and Gnatenco, 2001) and probably shares its properties. K_{2P}12.1 and K_{2P}15.1 may form functional heterodimers with unknown subunits.

The complex regulatory properties of these potassium channels may account for the effects of sustained stimulation and of the environment on the vestibular discharge. In the neuronal

somata and terminals, these channels are responsible for setting the resting membrane potential and electrical conductance, thus determine their excitability and discharge. Modulating these channels can modify the electrical properties of neurites thus their response to synaptic input. Thus, inhibition of $K_{2P}2.1$ in nerve terminals by type 1 metabotropic glutamate receptors, which are expressed in the crista ampullaris (in preparation), increases their excitability. Nerve terminals in the crista, which have $K_{2P}2.1$ and type 1 metabotropic glutamate receptors may show a slow buildup of activity upon stimulated release of glutamate by hair cells (as in Figure 4 and Figure 5 in Goldberg and Fernandez, 1971 or return to a higher resting discharge level than before stimulation (Fernandez et al., 1971).

$K_{2P}6.1$ in hair cells may explain the increase in afferent discharge by heat (Minor and Goldberg, 1990; von Baumgarten et al., 1984). Heat-inactivation of $K_{2P}6.1$ depolarizes the hair cells thus increasing the release of glutamate. Similarly, $K_{2P}3.1$ in supporting cells may explain the increase of the afferent discharge by high pH (Vega et al., 2003). An important role of supporting cells is K^+ recycling. K^+ enters hair cells through apical mechanosensory channels and exits by K^+ channels located on their basolateral region. Activation of $K_{2P}3.1$ in the supporting cells' lateral membrane by high external pH will facilitate diffusion of K^+ down its concentration gradient into the extracellular space leading to depolarization of nerve terminals and hair cells (Frankenhaeuser et al., 1956).

$K_{2P}2.1$ and $K_{2P}3.1$ in the vestibular periphery, may also mediate the effects of chronic exposure to volatile anesthetics on balance control. Chronic exposure to volatile anesthetics impairs the ability to regulate balance control from vestibule-proprioceptive information (Vouriot et al., 2005). In addition to central effects of volatile anesthetics, alteration of the resting discharge of the vestibular afferents due to activation of $K_{2P}2.1$ and $K_{2P}3.1$ in the vestibular periphery, may also contribute to impaired balance control.

$K_{2P}1.1$, $K_{2P}2.1$ and $K_{2P}3.1$ immunoreactivity was observed in dark cells and transitional cells. Dark cells are involved in endolymph secretion and homeostasis. Similar to their role in the nephron (Nie et al., 2005), these channels may mediate K^+ fluxes into the ampullae and in regulating the volume of endolymph. Because of their regulatory properties, these channels may mediate the influence of temperature, pH and increased pressure due to increased volume of endolymph on endolymph secretion. However, these phenomena have not yet been investigated, particularly in the context of inner ear disorders producing endolymphatic hydrops.

In conclusion, two-pore K^+ channels determine the electrical properties of neurons in the vestibular periphery and due to their complex regulatory properties may mediate the effect of the environment on the vestibular discharge and endolymph homeostasis.

Acknowledgments

Supported by NIH/NIDCD grants R01DC02971 (PAW) and R03DC006571 (PP), and intramural funds from the Toohill Research Fund of the Department of Otolaryngology and Communication Sciences, Medical College of Wisconsin, Milwaukee, Wisconsin.

References

Buckler KJ, Williams BA, Honore E. An oxygen-, acid- and anaesthetic-sensitive TASK-like background potassium channel in rat arterial chemoreceptor cells. J Physiol 2000;525(Pt 1):135–142. [PubMed: 10811732]

Charpak S, Gahwiler BH, Do KQ, Knopfel T. Potassium conductances in hippocampal neurons blocked by excitatory amino-acid transmitters. Nature 1990;347:765–767. [PubMed: 2172830]

Chavez RA, Gray AT, Zhao BB, Kindler CH, Mazurek MJ, Mehta Y, Forsayeth JR, Yost CS. TWIK-2, a new weak inward rectifying member of the tandem pore domain potassium channel family. J Biol Chem 1999;274:7887–7892. [PubMed: 10075682]

Chemin J, Girard C, Duprat F, Lesage F, Romey G, Lazdunski M. Mechanisms underlying excitatory effects of group I metabotropic glutamate receptors via inhibition of 2P domain K+ channels. Embo J 2003;22:5403–5411. [PubMed: 14532113]

Dechesne CJ, Winsky L, Kim HN, Goping G, Vu TD, Wenthold RJ, Jacobowitz DM. Identification and ultrastructural localization of a calretinin-like calcium-binding protein (protein 10) in the guinea pig and rat inner ear. Brain Res 1991;560:139–148. [PubMed: 1722130]

Desai SS, Ali H, Lysakowski A. Comparative morphology of rodent vestibular periphery. II. Cristae ampullares. J Neurophysiol 2005;93:267–280. [PubMed: 15240768]

Duprat F, Lauritzen I, Patel A, Honore E. The TASK background K(2P) channels: chemo- and nutrient sensors. Trends Neurosci 2007;30:573–580. [PubMed: 17945357]

Duprat F, Lesage F, Fink M, Reyes R, Heurteaux C, Lazdunski M. TASK, a human background K+ channel to sense external pH variations near physiological pH. Embo J 1997;16:5464–5471. [PubMed: 9312005]

Fernandez C, Goldberg JM. Physiology of peripheral neurons innervating semicircular canals of the squirrel monkey. II. Response to sinusoidal stimulation and dynamics of peripheral vestibular system. J Neurophysiol 1971;34:661–675. [PubMed: 5000363]

Fink M, Duprat F, Lesage F, Reyes R, Romey G, Heurteaux C, Lazdunski M. Cloning, functional expression and brain localization of a novel unconventional outward rectifier K+ channel. Embo J 1996;15:6854–6862. [PubMed: 9003761]

Frankenhaeuser B, Hodgkin AL. The after-effects of impulses in the giant nerve fibres of Loligo. J Physiol 1956;131:341–376. [PubMed: 13320339]

Goldberg JM, Fernandez C. Physiology of peripheral neurons innervating semicircular canals of the squirrel monkey. I. Resting discharge and response to constant angular accelerations. J Neurophysiol 1971;34:635–660. [PubMed: 5000362]

Goldstein SA, Bayliss DA, Kim D, Lesage F, Plant LD, Rajan S. International Union of Pharmacology. LV. Nomenclature and molecular relationships of two-P potassium channels. Pharmacol Rev 2005;57:527–540. [PubMed: 16382106]

Hasson T, Gillespie PG, Garcia JA, MacDonald RB, Zhao Y, Yee AG, Mooseker MS, Corey DP. Unconventional myosins in inner-ear sensory epithelia. J Cell Biol 1997;137:1287–1307. [PubMed: 9182663]

Heurteaux C, Guy N, Laigle C, Blondeau N, Duprat F, Mazzuca M, Lang-Lazdunski L, Widmann C, Zanzouri M, Romey G, Lazdunski M. TREK-1, a K+ channel involved in neuroprotection and general anesthesia. Embo J 2004;23:2684–2695. [PubMed: 15175651]

Honore E. The neuronal background K2P channels: focus on TREK1. Nat Rev Neurosci 2007;8:251–261. [PubMed: 17375039]

Jiang YQ, Oblinger MM. Differential regulation of beta III and other tubulin genes during peripheral and central neuron development. J Cell Sci 1992;103(Pt 3):643–651. [PubMed: 1478962]

Kang D, Choe C, Kim D. Thermosensitivity of the two-pore domain K+ channels TREK-2 and TRAAK. J Physiol 2005;564:103–116. [PubMed: 15677687]

Kanjhan R, Balke CL, Housley GD, Bellingham MC, Noakes PG. Developmental expression of two-pore domain K+ channels, TASK-1 and TREK-1, in the rat cochlea. Neuroreport 2004;15:437–441. [PubMed: 15094499]

Kim D, Gnatenco C. TASK-5, a new member of the tandem-pore K(+) channel family. Biochem Biophys Res Commun 2001;284:923–930. [PubMed: 11409881]

Krapivinsky G, Gordon EA, Wickman K, Velimirovic B, Krapivinsky L, Clapham DE. The G-protein-gated atrial K+ channel IKACh is a heteromultimer of two inwardly rectifying K(+)-channel proteins. Nature 1995;374:135–141. [PubMed: 7877685]

Lauritzen I, Blondeau N, Heurteaux C, Widmann C, Romey G, Lazdunski M. Polyunsaturated fatty acids are potent neuroprotectors. Embo J 2000;19:1784–1793. [PubMed: 10775263]

Leonard RB, Kevetter GA. Molecular probes of the vestibular nerve. I. Peripheral termination patterns of calretinin, calbindin and peripherin containing fibers. Brain Res 2002;928:8–17. [PubMed: 11844467]

Lesage F. Pharmacology of neuronal background potassium channels. Neuropharmacology 2003;44:1–7. [PubMed: 12559116]

Lesage F, Lazdunski M. Molecular and functional properties of two-pore-domain potassium channels. Am J Physiol Renal Physiol 2000;279:F793–F801. [PubMed: 11053038]

Lesage F, Guillemare E, Fink M, Duprat F, Lazdunski M, Romey G, Barhanin J. TWIK-1, a ubiquitous human weakly inward rectifying K+ channel with a novel structure. Embo J 1996;15:1004–1011. [PubMed: 8605869]

Maingret F, Patel AJ, Lazdunski M, Honore E. The endocannabinoid anandamide is a direct and selective blocker of the background K(+) channel TASK-1. Embo J 2001;20:47–54. [PubMed: 11226154]

Maingret F, Patel AJ, Lesage F, Lazdunski M, Honore E. Mechano- or acid stimulation, two interactive modes of activation of the TREK-1 potassium channel. J Biol Chem 1999;274:26691–26696. [PubMed: 10480871]

Maingret F, Lauritzen I, Patel AJ, Heurteaux C, Reyes R, Lesage F, Lazdunski M, Honore E. TREK-1 is a heat-activated background K(+) channel. Embo J 2000;19:2483–2491. [PubMed: 10835347]

Mhatre AN, Li J, Chen AF, Yost CS, Smith RJ, Kindler CH, Lalwani AK. Genomic structure, cochlear expression, and mutation screening of KCNK6, a candidate gene for DFNA4. J Neurosci Res 2004;75:25–31. [PubMed: 14689445]

Millar JA, Barratt L, Southan AP, Page KM, Fyffe RE, Robertson B, Mathie A. A functional role for the two-pore domain potassium channel TASK-1 in cerebellar granule neurons. Proc Natl Acad Sci U S A 2000;97:3614–3618. [PubMed: 10725353]

Miller P, Kemp PJ, Peers C. Structural requirements for O2 sensing by the human tandem-P domain channel, hTREK1. Biochem Biophys Res Commun 2005;331:1253–1256. [PubMed: 15883010]

Minor LB, Goldberg JM. Influence of static head position on the horizontal nystagmus evoked by caloric, rotational and optokinetic stimulation in the squirrel monkey. Exp Brain Res 1990;82:1–13. [PubMed: 2257895]

Nicolas MT, Barhanin J, Reyes R, Dememes D. Cellular localization of TWIK-1, a two-pore-domain potassium channel in the rodent inner ear. Hear Res 2003;181:20–26. [PubMed: 12855359]

Nicolas MT, Lesage F, Reyes R, Barhanin J, Dememes D. Localization of TREK-1, a two-pore-domain K+ channel in the peripheral vestibular system of mouse and rat. Brain Res 2004;1017:46–52. [PubMed: 15261098]

Nicoll RA, Malenka RC, Kauer JA. Functional comparison of neurotransmitter receptor subtypes in mammalian central nervous system. Physiol Rev 1990;70:513–565. [PubMed: 1690904]

Nie X, Arrighi I, Kaissling B, Pfaff I, Mann J, Barhanin J, Vallon V. Expression and insights on function of potassium channel TWIK-1 in mouse kidney. Pflugers Arch 2005;451:479–488. [PubMed: 16025300]

Patel AJ, Honore E. Properties and modulation of mammalian 2P domain K+ channels. Trends Neurosci 2001;24:339–346. [PubMed: 11356506]

Patel AJ, Lazdunski M. The 2P-domain K+ channels: role in apoptosis and tumorigenesis. Pflugers Arch 2004;448:261–273. [PubMed: 15133669]

Patel AJ, Honore E, Lesage F, Fink M, Romey G, Lazdunski M. Inhalational anesthetics activate two-pore-domain background K+ channels. Nat Neurosci 1999;2:422–426. [PubMed: 10321245]

Patel AJ, Maingret F, Magnone V, Fosset M, Lazdunski M, Honore E. TWIK-2, an inactivating 2P domain K+ channel. J Biol Chem 2000;275:28722–28730. [PubMed: 10887187]

Patel AJ, Honore E, Maingret F, Lesage F, Fink M, Duprat F, Lazdunski M. A mammalian two pore domain mechano-gated S-like K+ channel. Embo J 1998;17:4283–4290. [PubMed: 9687497]

Rajan S, Wischmeyer E, Karschin C, Preisig-Muller R, Grzeschik KH, Daut J, Karschin A, Derst C. THIK-1 and THIK-2, a novel subfamily of tandem pore domain K+ channels. J Biol Chem 2001;276:7302–7311. [PubMed: 11060316]

Reyes R, Duprat F, Lesage F, Fink M, Salinas M, Farman N, Lazdunski M. Cloning and expression of a novel pH-sensitive two pore domain K+ channel from human kidney. J Biol Chem 1998;273:30863–30869. [PubMed: 9812978]

Talley EM, Lei Q, Sirois JE, Bayliss DA. TASK-1, a two-pore domain K+ channel, is modulated by multiple neurotransmitters in motoneurons. Neuron 2000;25:399–410. [PubMed: 10719894]

Talley EM, Sirois JE, Lei Q, Bayliss DA. Two-pore-Domain (KCNK) potassium channels: dynamic roles in neuronal function. Neuroscientist 2003;9:46–56. [PubMed: 12580339]

Terrenoire C, Lauritzen I, Lesage F, Romey G, Lazdunski M. A TREK-1-like potassium channel in atrial cells inhibited by beta-adrenergic stimulation and activated by volatile anesthetics. Circ Res 2001;89:336–342. [PubMed: 11509450]

Vega R, Mercado F, Chavez H, Limon A, Almanza A, Ortega A, Perez ME, Soto E. pH modulates the vestibular afferent discharge and its response to excitatory amino acids. Neuroreport 2003;14:1327–1328. [PubMed: 12876466]

von Baumgarten R, Benson A, Berthoz A, Brandt T, Brand U, Bruzek W, Dichgans J, Kass J, Probst T, Scherer H, et al. Effects of rectilinear acceleration and optokinetic and caloric stimulations in space. Science 1984;225:208–212. [PubMed: 6610216]

Vouriot A, Gauchard GC, Chau N, Nadif R, Mur JM, Perrin PP. Chronic exposure to anesthetic gases affects balance control in operating room personnel. Neurotoxicology 2005;26:193–198. [PubMed: 15713340]

Wackym, PA. Hearing and Balance Gene Expression Database. [accessed July 31, 2008]. URL: http://www.genexpression.info

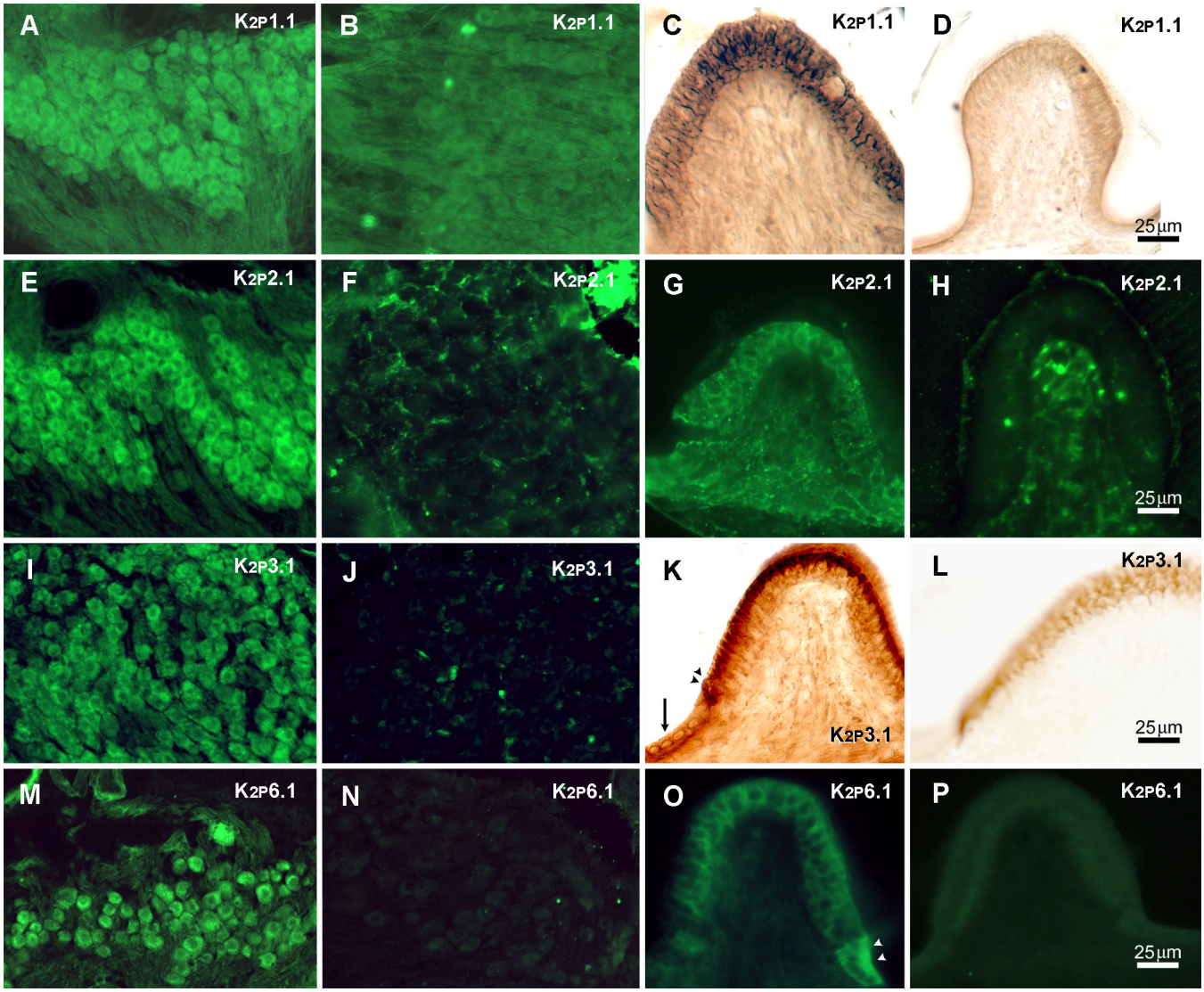

Fig. 1.

$K_{2P}1.1$, $K_{2P}2.1$, $K_{2P}3.1$ and $K_{2P}6.1$ immunoreactivity in 40 μm sections of Scarpa's ganglia (**A, E, I, M**) and cristae ampullares (**C, G, K, O**) are shown. **B, F, J, N** and **D, H, L, P** show 40 μm sections of ganglia and cristae, respectively processed with the antibodies preabsorbed with the immunizing peptides, and significantly reduced staining. In panels **C, D, K** and **L** the chromogen was diaminobenzidene and in the others Alexa-488. Large arrow point to vestibular dark cells and arrowheads point to transitional cells. Scale bar=25 μm.

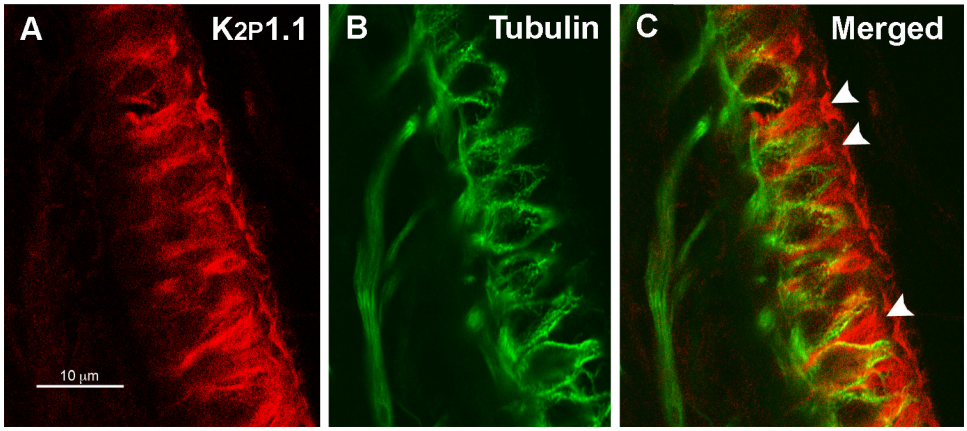

Fig. 2.

Magnified single confocal images of a 40 μm thick section of a crista ampullaris processed for $K_{2P}1.1$ (red) and tubulin β III (green) immunoreactivity. The yellow color on the merged image indicates co-localization of $K_{2P}1.1$ and tubulin immunoreactivity within some of the nerve terminals. The arrowheads point to supporting cells immunolabeled with $K_{2P}1.1$. Scale bar=10 μm.

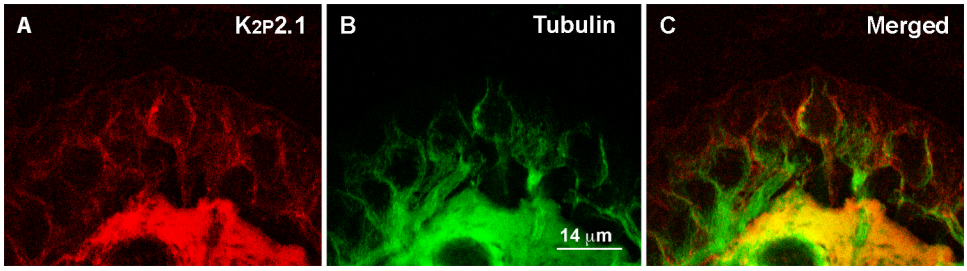

Fig. 3.

Magnified single confocal images of a 40 μm thick section of a crista ampullaris processed for $K_{2P}2.1$ (red) and tubulin β III (green) immunoreactivity. $K_{2P}2.1$ immunoreactivity is localized to nerve terminals. The yellow color on the merged image indicates co-localization of $K_{2P}2.1$ and tubulin immunoreactivity within some of the nerve terminals. Scale bar=14 μm.

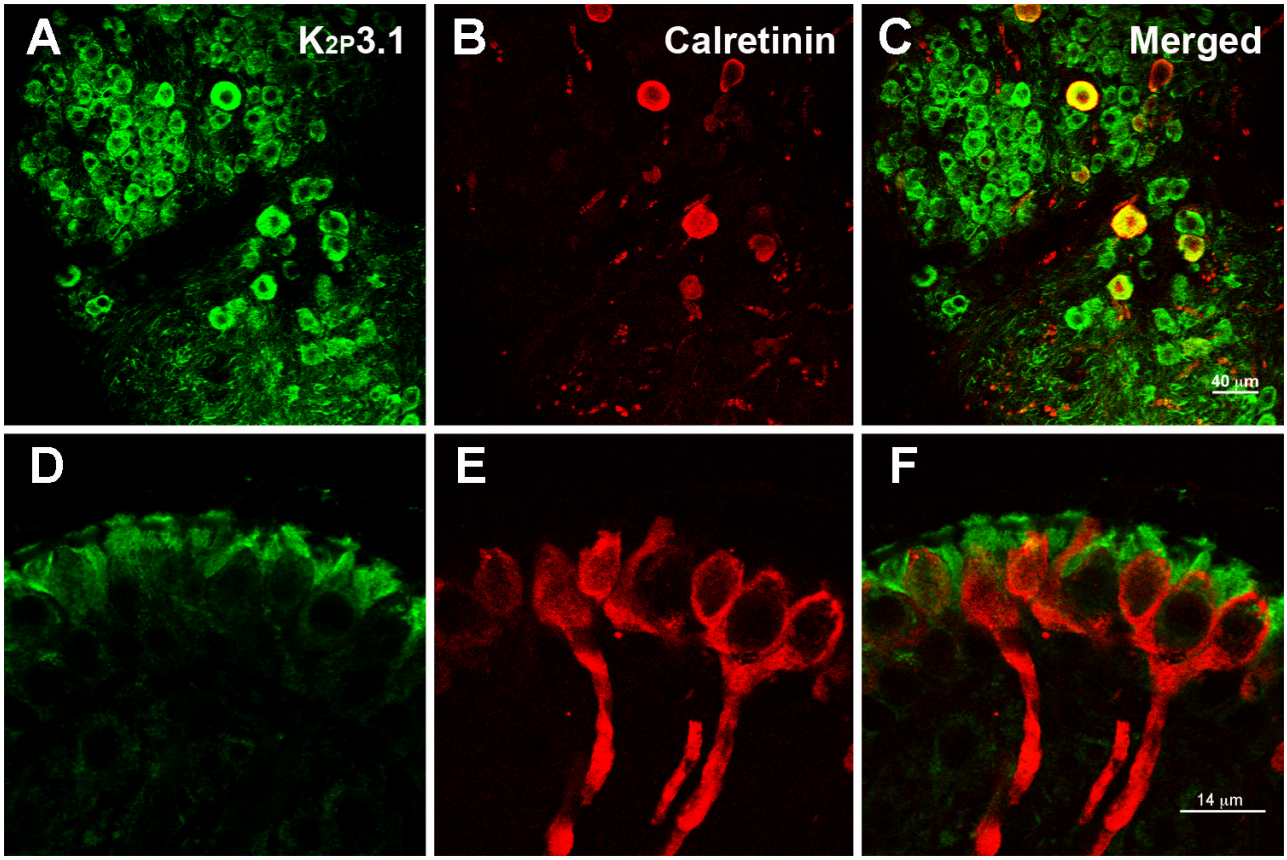

Fig. 4.

Single confocal images of a 40μm thick section of a Scarpa's ganglion processed for $K_{2P}3.1$ (green) and calretinin (red) immunoreactivity (**A, B, C**). The yellow color on the merged image indicates co-localization of $K_{2P}3.1$ and calretinin in some of the caliceal primary afferent neurons. Scale bar=40 μm. **Bottom row**. Magnified single confocal images of a 40 μm thick section of a crista ampullaris processed for $K_{2P}3.1$ (green) and calretinin (red) immunoreactivity (**D, E, F**). $K_{2P}3.1$ immunoreactivity can be seen in supporting cells. There is no co-localization of $K_{2P}3.1$ immunoreactivity in calretinin immunoreactive calices, although there is co-localization in some of the somata as shown in (**C**). Scale bar=14 μm.

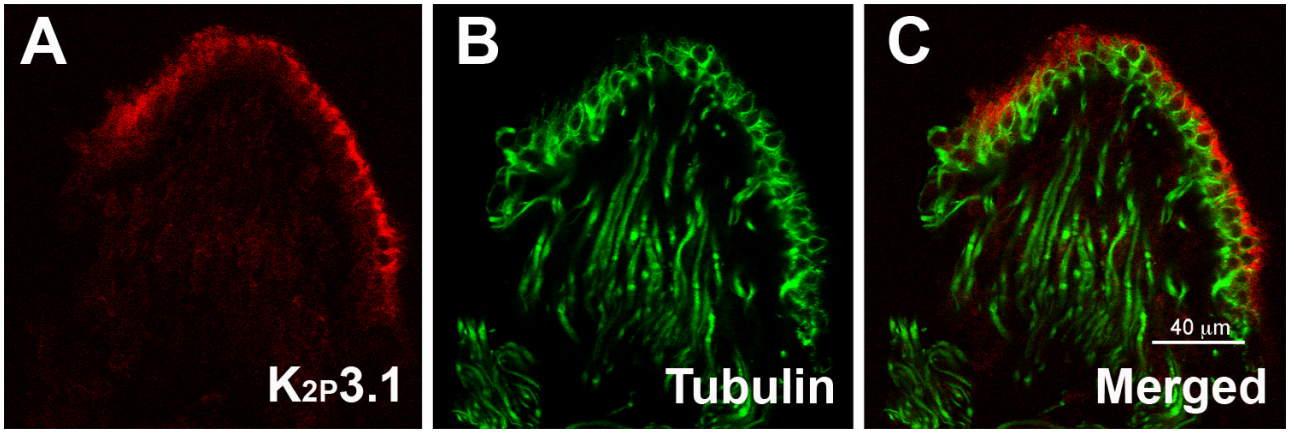

Fig. 5.

Single confocal images of a 40 µm thick section of a crista ampullaris processed for $K_{2P}3.1$ (red) and tubulin β III (green) immunoreactivity. $K_{2P}3.1$ immunoreactivity is localized to the apical portion of supporting cells and the absence of yellow on the merged image indicates no co-localization of tubulin immunoreactivity in primary afferent terminals. Scale bar=40 µm.

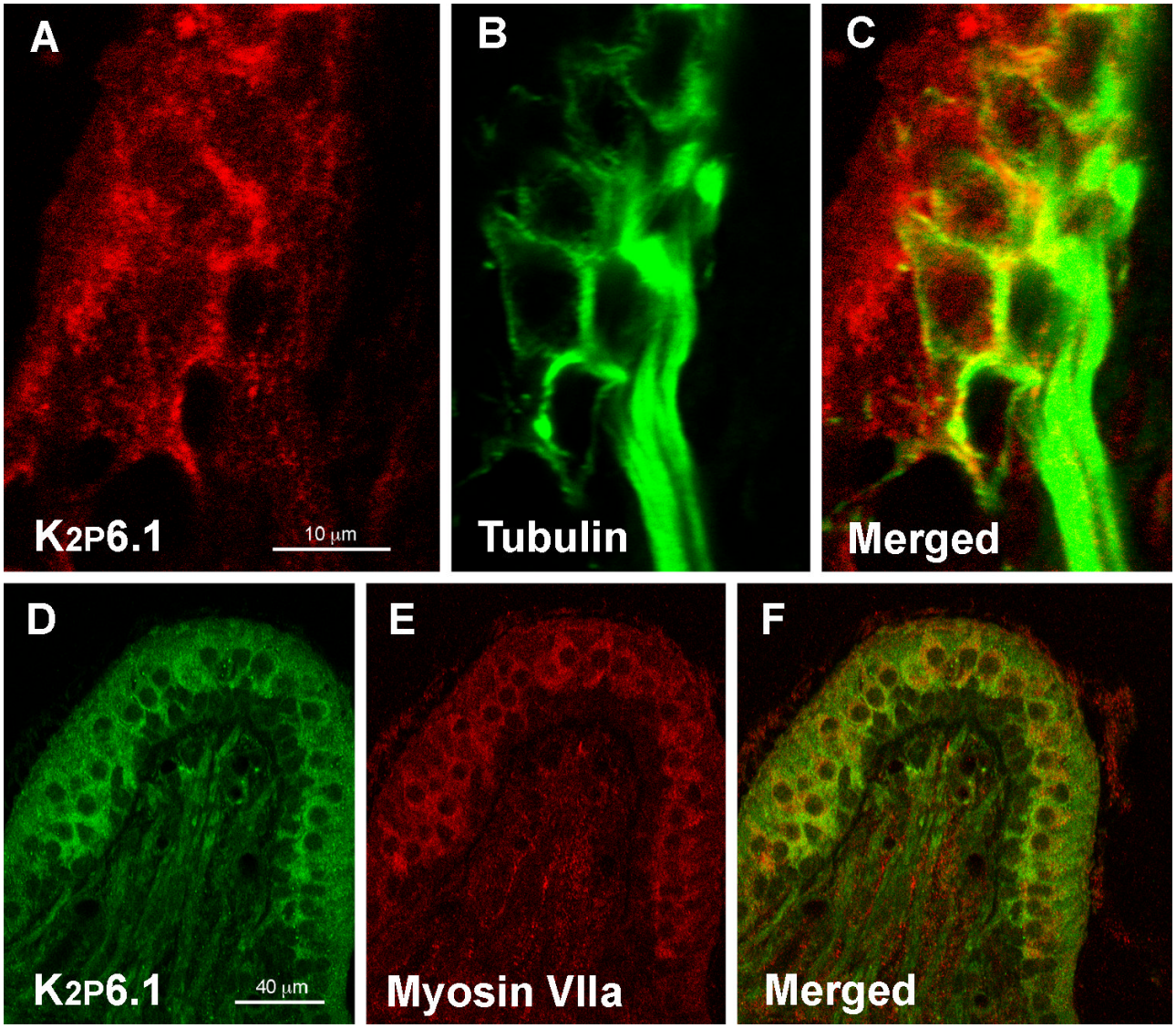

Fig. 6.

Magnified single confocal images of a 40 μm thick section of a crista ampullaris processed for $K_{2P}6.1$ (red) and tubulin β III (green) immunoreactivity (**A, B, C**). $K_{2P}6.1$ is localized to primary afferent nerve terminals and the yellow color on the merged image indicates co-localization of tubulin immunoreactivity in primary afferent terminals. Scale bar=10 μm. **Bottom row**. Single confocal images of a 40 μm thick section of a crista ampullaris processed for $K_{2P}6.1$ (green) and myosin VIIa (red) immunoreactivity (**D, E, F**). The merged image shows that $K_{2P}6.1$ immunoreactivity is also in vestibular hair (**F**). Scale bar=40 μm.

TABLE 1

Two-pore-domain potassium channel gene symbol, nomenclature, anatomic distribution and expression level measured using real-time PCR expression.*

			Expression Level	
Gene Symbol	**Previous Nomenclature**	**Current Nomenclature**	**Ganglia**	**Crista Ampullares**
Kcnk1	TWIK-1	$K_{2p}1.1$	1.24 ± 2.16	1.24 ± 1.66
Kcnk2	TREK-1	$K_{2p}2.1$	0.88 ± 2.4	0.81 ± 1.96
Kcnk3	TASK-1	$K_{2p}3.1$	4.63 ± 1.20	10.54 ± 1.55
Kcnk6	TWIK-2	$K_{2p}6.1$	2.07 ± 2.38	3.84 ± 1.46
Kcnk12	THIK-2	$K_{2p}12.1$	4.31 ± 1.57	2.89 ± 0.41
Kcnk15	TASK-5	$K_{2p}15.1$	9.76 ± 2.44	Not expressed

*Expression level of these genes, relative to the expression of hypoxanthine guanine phosphoribosyl transferase (HPRT) in the Scarpa's ganglia and in the crista ampullares were calculated as the average number of cycles needed to reach threshold compared to HPRT (mean ΔC_T).

TABLE 2

Immunohistochemical distribution of two-pore-domain potassium channels in the vestibular periphery.

	$K_{2P}1.1$	$K_{2P}2.1$	$K_{2P}3.1$	$K_{2P}6.1$
Ganglion neurons	+	+	+	+
Afferent terminals	+	+	−	+
Hair cells	−	−	−	+
Supporting cells	+	−	+	−
Transitional cells	−	+	+	+
Dark cells	+	+	+	−